Single-Molecule Magnets

DOI: 10.1002/ange.200704460

Single-Molecule Magnets with Mesomorphic Lamellar Ordering**

Emmanuel Terazzi, Cyril Bourgogne, Richard Welter, Jean-Louis Gallani, Daniel Guillon, Guillaume Rogez, and Bertrand Donnio**

Single-molecule magnets (SMMs) are materials that are able to retain magnetization at the molecular level below a certain temperature, known as the blocking temperature.[1,2] These compounds currently elicit sustained research activity: as quantum objects they are envisioned as qubits for quantum computers, and their magnetic properties make them the ultimate storage bits of a molecular magnetic memory. Schematically, these hybrid molecules are made from metal ions bound together by various organic ligands, and numerous types of compounds have been reported to show SMM behavior: 4f coordination compounds,[3] polymetallic cages,[4] and oxometallaclusters.[2,5] Despite its poor stability against water and temperature, the so-called "Mn_{12}" compound $[Mn_{12}O_{12}(OAc)_{16}(H_2O)_4]$ is probably the most studied SMM for at least two reasons: its synthesis is cheap and easy, and it long held the record for the highest blocking temperature.[2b]

The use of functional molecules in macroscopic devices (bottom-up technology) requires that some degree of low-dimensionality self-organization (1D or 2D) is imparted to the molecules. It is well known that self-organization can only take place in a system that has some fluidity during the process so that positioning errors can be corrected automatically. Liquid crystals are a prime example of molecular assemblies in which order coexists with fluidity.[6]

We describe herein how dedicated design can endow the Mn_{12} molecule with liquid-crystalline (LC) properties while preserving the peculiar magnetic properties of the original core; a side effect of this added functionality is much improved thermal stability. The formation of positionally ordered mesophases is a first step on the route to organizing SMMs for their eventual incorporation in a functional nanodevice.

To counterbalance the a priori unfavorable molecular shape and bulkiness of the Mn_{12} cluster core and the important geometrical constraints, we applied the strategies used to obtain thermotropic mesophases with fullerenes (fulleromesogens[7]), bulky lanthanidomesogens,[8] octahedral coordination complexes,[9] or supramolecular objects.[10] The procedure consists of covalent grafting of either a mesomorphic promoter onto the inorganic cluster through a flexible aliphatic spacer[7,8b,10] or strongly lipophilic ligands[8a,9] to improve interfaces and areas compatibilities between both moieties and to enhance microsegregation.

Mesomorphic, dodecanuclear manganese complexes $[Mn_{12}O_{12}(O_2CR)_{16}(H_2O)_4]$ were thus obtained by the replacement of the 16 LC-inert acetate groups (R = Me) with gallate-derived moieties (Scheme 1). Depending on the chosen

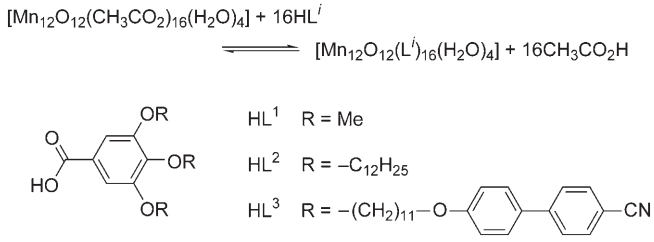

Scheme 1. Ligand exchange between $[Mn_{12}(OAc)_{16}]$ and HL^i to yield $[Mn_{12}L^i_{16}]$ complexes, and chemical structures of the gallic derivatives HL^1, HL^2, and HL^3.

benzoate, 1D (smectic) or 3D (body-centered cubic) organized mesophases were indeed induced. This is, to the best of our knowledge, the first example of liquid crystalline metallaclusters and as such opens new perspectives in the field of self-organized and ordered structures of SMMs.[11]

The three dodecanuclear complexes, abbreviated $[Mn_{12}L^i_{16}]$, were synthesized from $[Mn_{12}(OAc)_{16}]$ by ligand exchange between the acetate groups and the corresponding gallic acid derivatives with methoxy (HL^1), dodecyloxy (HL^2), or cyanobiphenyloxyundecyloxy (HL^3) groups (Scheme 1); $[Mn_{12}(OAc)_{16}]$ was prepared in situ from $MnOAc_2$ and $KMnO_4$, and the gallic acid derivatives HL^2 and HL^3 were prepared by following published procedures.[8,9]

The characterization of the final compounds relied mostly on elemental analysis and IR spectroscopy, as NMR spectroscopy was not suitable on account of the three paramagnetic clusters. The covalent grafting and the complete substitution of the 16 positions by the benzoates onto the clusters was confirmed by the disappearance of the stretching

[*] Dr. E. Terazzi, Dr. C. Bourgogne, Dr. J.-L. Gallani, Dr. D. Guillon, Dr. G. Rogez, Dr. B. Donnio
Institut de Physique et Chimie des Matériaux de Strasbourg (IPCMS)
UMR7504 (CNRS-Université Louis Pasteur Strasbourg)
23 rue du Lœss, BP 43, 67034, Strasbourg cedex 2 (France)
Fax: (+33) 388-107-246
E-mail: rogez@ipcms.u-strasbg.fr
bdonnio@ipcms.u-strasbg.fr
Homepage: http://www-ipcms.u-strasbg.fr/
Prof. R. Welter
Laboratoire DECOMET
UMR7177 (CNRS-Université Louis Pasteur Strasbourg)
4 rue Blaise Pascal, 67070 Strasbourg cedex (France)

[**] We are grateful to the Swiss National Science Foundation, the CNRS-ULP, and the National Agency for Research (ANR DENDRIMAT) for financial support. We thank N. Beyer for the artwork, D. Burger for TGA measurements, and Dr. B. Heinrich for discussions.

Supporting information for this article is available on the WWW under http://www.angewandte.org or from the author.

vibration of the carbonyl groups of the free benzoates HL^1 to HL^3; this absence also indicated that no free ligand or acetate is present (see Figures S1–S3 in the Supporting Information). Elemental analyses were in agreement with the proposed structures (see Table S1 in the Supporting Information). Also, cocrystallised solvent molecules were confirmed by TG measurements (see Figures S4–S6 in the Supporting Information).

We were able to obtain the single-crystal X-ray structure of the model compound $[Mn_{12}L^1{}_{16}]$, which allowed us to check the bonding mode of the benzoate groups on the oxocluster. The compound crystallizes in the $P\bar{1}$ space group with two formula units in the unit cell,[12] and the structure is similar to that of previously described Mn_{12} complexes (see Figure S12 in the Supporting Information).[13] It consists of a roughly planar disk made up of a central $Mn^{IV}{}_4O_4$ cube surrounded by a ring of eight Mn^{III} centers connected to the cube by eight μ_3-O^{2-} and four κ^2-μ_2-carboxylate groups perpendicular to the plane of the disk (two on each side). Furthermore, the peripheral Mn^{III} centers are connected to each other by eight equatorial and four axial κ^2-μ_2-carboxylate groups. Two types of Mn^{III} ions can be distinguished: type I, doubly bridged to one Mn^{IV} center; and type II, singly bridged to two Mn^{IV} centers. Four different isomers of Mn_{12} have been described in the literature: 1:1:1:1, 1:2:1:0, 1:1:2:0, and 2:2:0:0 (the notation indicates the number of water molecules coordinated to type II Mn^{III} ions).[2b] The present $[Mn_{12}L^1{}_{16}]$ compound corresponds to the 2:2:0:0 form, whereas the predominant isomer of $[Mn_{12}(OAc)_{16}]$ is the 1:1:1:1 form.[2]

The occurrence of a frequency-dependent out-of-phase ac susceptibility signal (χ'') is considered a signature for SMM properties.[2,14] In an ac susceptibility measurement, an out-of-phase signal (χ'') is expected to appear if the relaxation frequency of the magnetization of the sample becomes close to the frequency of the ac field. Moreover, ac magnetic susceptibility can be used to determine the spin of the ground state and the effective energy barrier (U_{eff}) for the relaxation of magnetization. Figure 1 shows plots of $\chi'T$ versus T and χ'' versus T at various frequencies. The frequency-dependent decrease in the $\chi'T$ versus T plot on lowering the temperature indicates that the relaxation of the magnetization rate becomes close to the ac field frequency. Accordingly, a χ'' signal appears at the corresponding temperature, indicating SMM behavior of the samples.

For the three compounds, the $\chi'T$ values above 8 K are equal and constant at all frequencies. Assuming that only the ground state is populated at this temperature, the value of $\chi'T$ can be used to determine the spin of the ground state of the clusters. For $[Mn_{12}L^1{}_{16}]$, the value of $\chi'T$ at the plateau is around 51 emu K mol^{-1}, which corresponds to a ground state of $S=10$ and $g=1.93$. For $[Mn_{12}L^2{}_{16}]$, the value of $\chi'T$ at the plateau (ca. 42 emu K mol^{-1}) leads to $S=9$ and $g=1.94$, and, for $[Mn_{12}L^3{}_{16}]$, to $S=9$ and $g=1.91$ ($\chi'T\approx41$ emu K mol^{-1}). These values are in accordance with the values determined for other Mn_{12} complexes: although most complexes possess a spin ground state of $S=10$, a ground state of $S=9$ was observed with propionate,[13d] benzoate,[13c,15a] and *meta*-chlorobenzoate[15b] ligands. These results, determined from ac susceptibility measurements, are in accordance with

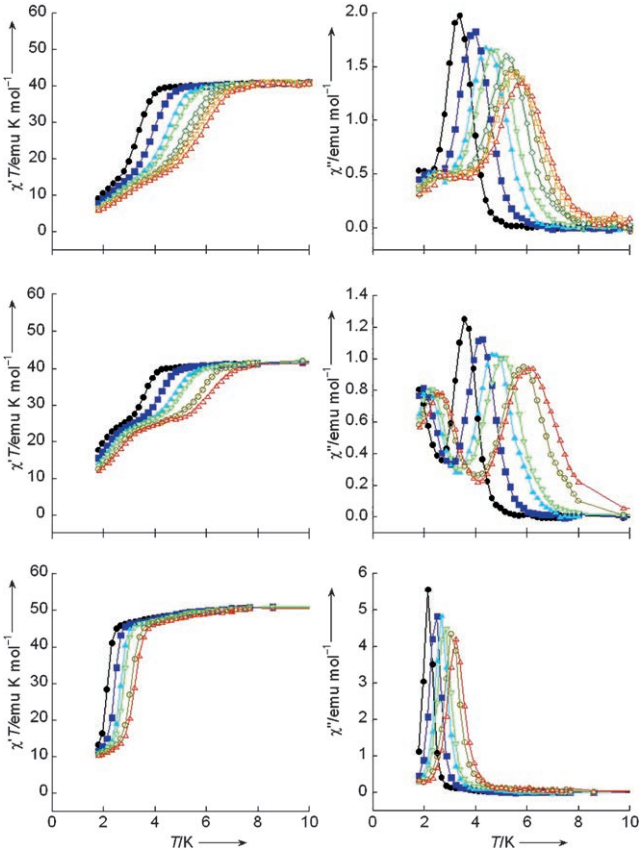

Figure 1. Temperature dependence of $\chi'T$ (left) and χ'' (right) for $[Mn_{12}L^1{}_{16}]$ (bottom), $[Mn_{12}L^2{}_{16}]$ (middle), and $[Mn_{12}L^3{}_{16}]$ (top). χ' and χ'' are the real and imaginary components of the molar magnetic susceptibility at zero dc field with a field of 3.5 Oe oscillating at 1000 (△), 750 (□), 500 (○), 300 (◇), 100 (▽), 50 (▲), 10 (■), and 1 Hz (●).

$[Mn_{12}L^1{}_{16}]$ presenting a higher high-field magnetization value than $[Mn_{12}L^2{}_{16}]$ and $[Mn_{12}L^3{}_{16}]$ (see below). Whereas $[Mn_{12}L^1{}_{16}]$ exhibits a frequency-dependent out-of-phase signal in the region 2–4 K, $[Mn_{12}L^2{}_{16}]$ presents two signals, one in the region 4–7 K, the other in the region 2–4 K, and $[Mn_{12}L^3{}_{16}]$ presents essentially one out-of-phase signal in the region 4–7 K (a low-temperature peak is actually present but not clearly visible).

The possible occurrence of two peaks in out-of-phase susceptibility is not an unusual feature for Mn_{12} derivatives. Actually, the parent $[Mn_{12}(OAc)_{16}]$ complex exhibits only one frequency-dependent out-of-phase signal in the region 4–7 K,[2c] but it has long been observed that some Mn_{12} derivatives may present two signals, one in the region 4–7 K, the other in the region 2–4 K, or only the low-temperature signal.[13d,16,17] The origin of these two relaxation processes has been attributed to Jahn–Teller isomerism: for $[Mn_{12}(OAc)_{16}]$, all the Jahn–Teller elongation axes of the peripheral Mn^{III} centers are oriented perpendicularly to the plane of the molecule, whereas for systems that present the low-temperature χ'' peak, it has been shown that one of the peripheral Mn^{III} ions had an unusual orientation of its Jahn–Teller elongation axis, almost perpendicular to the elongation axis of the other Mn^{III} center. This Jahn–Teller isomerism is responsible for the lowering of the temperature at which the

molecule experiences slow relaxation of the magnetization (blocking temperature), provoking an overall lowering of the magnetic anisotropy of the molecule (a key parameter for the slow relaxation process) and favoring the occurrence of rhombic (transverse) zero-field interactions within the molecules. This results in an increase of the rate of the reversal of the magnetization by quantum tunneling.[13d] A closer examination of the crystal structure of $[Mn_{12}L^{1}{}_{16}]$ shows that one of the Mn^{III} ions has a Jahn–Teller elongation axis almost perpendicular to the others (see Figure S12 in the Supporting Information). In view of the very low disorder of the crystal structure ($R_1 = 6.1\,\%$), this Jahn–Teller-distorted isomer is the only one significantly present in the structure, which explains the occurrence of a unique out-of-phase signal at a lower temperature than for the parent $[Mn_{12}(OAc)_{16}]$ compound. For $[Mn_{12}L^{2}{}_{16}]$ and $[Mn_{12}L^{3}{}_{16}]$, for which no structure of the core is available, the presence of two peaks suggests the coexistence of different Jahn–Teller isomers within the sample, as already observed for other Mn_{12} derivatives.[13d]

For the three complexes, the magnetization relaxation rate τ follows an Arrhenius equation ($\tau = \tau_0 \exp(-U_{eff}/kT)$, see Figure S13 in the Supporting Information). This behavior is characteristic for a thermally activated Orbach process in which U_{eff} is the effective anisotropy energy barrier, k the Boltzmann constant, and τ_0 the preexponential factor. For $[Mn_{12}L^{2}{}_{16}]$ it was possible to extract the parameters for both phases, those corresponding to the high-temperature peak (slow relaxation phase, SR), and those of the low-temperature peak (fast relaxation phase, FR). The values obtained for the three complexes (Table S4 in the Supporting Information) all fall within the expected ranges for Mn_{12} complexes. The shape of the magnetization versus field curves at 1.8 K for the three compounds is typical for randomly oriented polycrystalline Mn_{12} species (Figure S14 in the Supporting Information).[17b] The magnetization curves of the three clusters exhibit a hysteresis loop characteristic of SMM behavior.[2b] The weak coercive field of 52 mT observed for $[Mn_{12}L^{1}{}_{16}]$ is in accordance with the very low T_B value (1.6 K), which is slightly below the temperature of measurement (1.8 K); T_B is arbitrarily defined as the temperature for which $\tau = 100$ s.[17a] For $[Mn_{12}L^{2}{}_{16}]$ ($\mu_0 H_C = 125$ mT), only the SR species show hysteresis behavior as T_B (FR) $< 1.8\,K < T_B$ (SR). The presence of the FR species leads to narrowing of the hysteresis loop at zero field measured for the sample.[17b] Finally, $[Mn_{12}L^{3}{}_{16}]$ shows a rather large coercive field of 320 mT, which is in accordance with its unique and high T_B value of 2.4 K.

Polarized optical microscopy (POM) and small- and wide-angle X-ray diffraction (SAXS) experiments show that $[Mn_{12}L^{1}{}_{16}]$ is solid (crystalline) until it decomposes at around 200 °C, whereas $[Mn_{12}L^{2}{}_{16}]$ and $[Mn_{12}L^{3}{}_{16}]$ are mesomorphic and thermally stable up to around 150 °C, where decomposition occurs before the clearing point is reached (Table 1).

No birefringent texture could be observed for $[Mn_{12}L^{2}{}_{16}]$ in the explored temperature range, but only the formation of large black (optically isotropic) viscous areas on increasing temperature above 25 °C. A cubic mesophase with a $Im\bar{3}m$ symmetry was eventually deduced from SAXS measurements. At 30 °C, up to 11 sharp reflections (Figure S9, Table S2, Supporting Information) were detected in the low-angle range for which the reciprocal d spacings were in the ratios $\sqrt{10}:\sqrt{12}:\sqrt{14}:\sqrt{16}:\sqrt{20}:\sqrt{22}:\sqrt{38}:\sqrt{40}:\sqrt{44}:\sqrt{48}:\sqrt{54}$, pointing to a cubic supramolecular organization $[(h^2+k^2+l^2)^{1/2} = a/d_{hkl})]$; the number of reflections decreased to 4–5 upon increasing temperature. A very intense and broad diffraction peak centered at around 4.5 Å (h_{ch}) was present over the whole temperature range, corresponding to the molten alkyl chains and confirming the liquid nature of the mesophase. Complete space group determination of mobile thermotropic cubic phases is difficult but important. The large initial number of theoretical possibilities (36) can be decreased by logical analysis of the data, as shown below. In our standard diffraction experiment, all non-centrosymmetric groups (groups with Laue classes 23, 432, or $-43m$) can be disregarded on account of Friedel's law,[18] which leaves only 17 cubic space groups to consider. The sequence of the ratios is not compatible with a face-centered cubic network (F), and, although it is still compatible with a primitive Bravais lattice (P), this option is highly improbable owing to the 10 or so absent authorized reflections and the consequently too large lattice parameter. The symmetry of the cubic phase is thus characterized by a body-centered cubic network (I) with a lattice parameter $a = 105.1$ Å. The reflections were indexed as (310), (222), (321), (400), (420), (332), (611/532), (620), 622), (444), and (633/552/721), and all satisfied the reflection conditions $0kl{:}k+l=2n$, $hhl{:}l=2n$, $h00h=2n$; only the symmetry of space groups $Im\bar{3}$ and $Im\bar{3}m$ is theoretically compatible with this set of reflections. Aggregation into the highest symmetry is generally admitted, and, accordingly, the $Im\bar{3}m$ space group is finally retained.[19,20] The cubic lattice parameter is almost temperature-independent ($a = 106.1$ Å at $T = 90$ °C and $a = 108.1$ Å at $T = 140$ °C). As deduced from the estimated molecular volume ($V_{mol} \approx 20000$–22000 Å^3, $\rho \approx 1.0$ g.cm^{-3}), the unit cell of the cubic phase (a^3) contains 55–60 molecular clusters.

Thermotropic cubic phases with the $Im\bar{3}m$ space group are rare in liquid crystals,[19,20] and their structure not clearly understood,[21] in contrast to their lyotropic analogues. Considering first the discontinuous micellar model, as for

Table 1: Temperatures and enthalpy and entropy changes of the phase transitions for MeL^3, HL^3, $[Mn_{12}L^{2}{}_{16}]$, and $[Mn_{12}L^{3}{}_{16}]$.

Compd	Mesophases[a,c]	T [°C]	ΔH [J g^{-1}]	ΔS [mJ g^{-1} K^{-1}]
MeL^3[b]	Cr→SmA	16.5	2.02	6.97
	SmA→N	85.2	0.24	0.67
	N→I	99.6	3.21	8.61
HL^3[b]	Cr→N	138.2	–	–
	N→I	141.1	78.49[d]	223.21[d]
$[Mn_{12}L^{2}{}_{16}]$	Cr→Cub	−11.5	24.06	91.95
	Cub→dec	150.0	–	–
$[Mn_{12}L^{3}{}_{16}]$	G→Sm_{fmr}	40.5	–	–
	Sm_{fmr}→dec	150.0	–	–

[a] Second heating; [b] Polarized optical microscopy (POM); [c] Cr = crystal, G = glass, I = isotropic liquid, SmA = smectic A, N = nematic, Cub = cubic, Sm_{fmr} = filled random mesh smectic phase (see text and reference [26]), dec = decomposition; [d] cumulative values for both transitions.

supramolecular dendromesogens,[19] two discrete, globular aggregates (see Figure S15 in the Supporting Information) with an aggregation number of 27–30 molecules would be formed and regularly organized in the three spatial directions. Such an ordered, periodic 3D array is, however, unlikely owing to weakly cohesive and nondirectional intermolecular and inter-"aggregate" interactions. Another, better, alternative for the description of the 3D organization would be to consider multicontinuous cubic structures made of two or three interwoven, infinite, interconnected columnar networks, each separated by lipophilic films (minimal surfaces) (see Figure S16 in the Supporting Information).[21] The fact that (321) and (400) are the dominant reflections in the powder X-ray pattern points preferentially to the $Im\bar{3}m$ (I) triple interpenetrated network model (as demonstrated in another study by direct Fourier reconstruction of electron density[21c]), although, a comprehensive explanation of the supramolecular organization is not yet possible.

In contrast, $[Mn_{12}L^3{}_{16}]$ exhibited a homogeneous and fluid birefringent optical texture from 40 °C upwards. The lack of characteristic defects precluded any visual determination, but X-ray diffraction scans as a function of temperature allowed the identification of the mesophase. Two equidistant sharp reflections were observed in the diffractogram in a ratio of 1:2 (42.3 and 21.0 Å, 00l reflections with $l = 1$, 2), which is indicative of lamellar order (Figure 2 and Table S3 in the

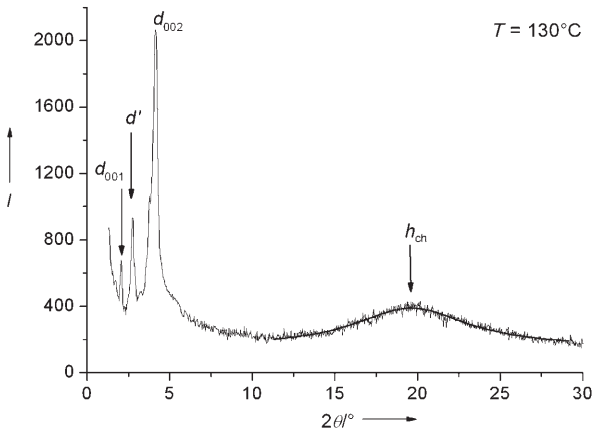

Figure 2. SAXS profile of the lamellar structures of $[Mn_{12}L^3{}_{16}]$.

Supporting Information). A broad and diffuse scattering, corresponding to the short-range order of the molten chains, was detected at 4.5 Å (h_{ch}). Another diffraction signal, at 28.5 ± 0.5 Å (d'), with a different line shape and not commensurate with the peaks of the lamellar structure was also present. This peak was assigned to some intralayer order associated with a specific arrangement of the diffracting centers, that is, the magnetic cores. The features of the peak (intensity relative to d_{002} and full width at half maximum) imply that this order is short-ranged and that the position of the diffracting centers is not correlated from layer to layer. Such an intralayer organization would be sterically induced by the bulky cyanobiphenyl groups. The intensity of the 001 reflection is weak relative to that of 002, implying a modulation of the electronic density within the lamellar periodicity. This result suggests organization in which the peripheral mesogenic groups are equally distributed on either side of the metallic cluster in a compact manner (cylindrical molecular conformation), resembling the microsegregated smectic structures formed by mesogenic end-capped dendrimers.[22] The interlayer periodicity d is almost invariant with temperature in the range 60–140 °C ($\langle d \rangle = 42.15$ Å). From the calculated molecular volume ($V_{mol} \approx 34000$–35000 Å^3, $\rho \approx 1.0$ g cm^{-3}), the molecular and mesogenic areas ($A_M = V_{mol}/d$ and $a_m = A_M/24$, respectively) could be estimated: $A_M \approx 810$–830 Å^2 and $a_m \approx 33.75$–34.6 Å^2. The latter value differs from the cross-sectional area of 22–24 Å^2 expected for a cyanobiphenyl group arranged normal to the smectic layer (SmA type). In this case, the sublayers containing the peripheral groups are either partially interdigitated, as in the case of the SmA_d phase,[23] or the aliphatic spacers and the cyanobiphenyl groups are tilted with an angle of about 50° but without any correlation in the tilt direction, as in the SmA phase of de Vries type.[24]

This supramolecular organization is validated by molecular dynamics simulations. A molecular model of a smectic bilayer was built with a cell height of 200 Å (larger than the measured value so as not to constrain the thickness artificially) and an area $S \approx 810$ Å^2 containing two superimposed molecules. As none of the available force fields for the molecular dynamics studies were able to simulate correctly the ring shape of the Mn_{12} cluster, each manganese atom of a given cluster was restricted to its position relative to the others, according to the X-ray diffraction structure of compound $[Mn_{12}L^1{}_{16}]$. All non-Mn atoms of the cluster are allowed to move freely, as were the two molecules in the cell. An average interlayer periodicity of 41.9 Å was obtained, which is in excellent agreement with the measured value (see Figure S19 in the Supporting Information). We also attempted to determine the nature of the aforementioned in-plane order with molecular modeling. Positional order in molecular 2D assemblies is most often hexagonal or squarelike.[25] For hexagonal packing of the Mn_{12} cores, the average distance between neighboring magnetic centers would then be 30.5 Å ($S = {}^1/_2 \times a_{Hex}{}^2 \times 3^{1/2}$), and the intralayer order would be 26.5 Å, which is smaller than the measured d' value (see Table S3 in the Supporting Information). However, if a squarelike pattern is considered, an average core-to-core distance of 28.4 Å ($\sqrt{S}$) is found, which is in better accordance with the experimental data (Figure 3). The intrinsic fourfold molecular cluster symmetry could favor the squarelike packing. In the fluid phase, both patterns are likely to coexist, with the square lattice prevailing over the hexagonal one.

Thus, this smectic arrangement can be described as follows: the two incompatible segments (mesogens and aliphatic spacers) form alternating layers, with tilt and interdigitation of the mesogens between successive periods, and the Mn_{12} cores are located in the aliphatic sublayers and arranged into a squarelike planar array. This supramolecular organization resembles that of the so-called "filled mesh phases" observed with some facial amphiphiles, in which ionic clusters (formed by the laterally attached alkali metal

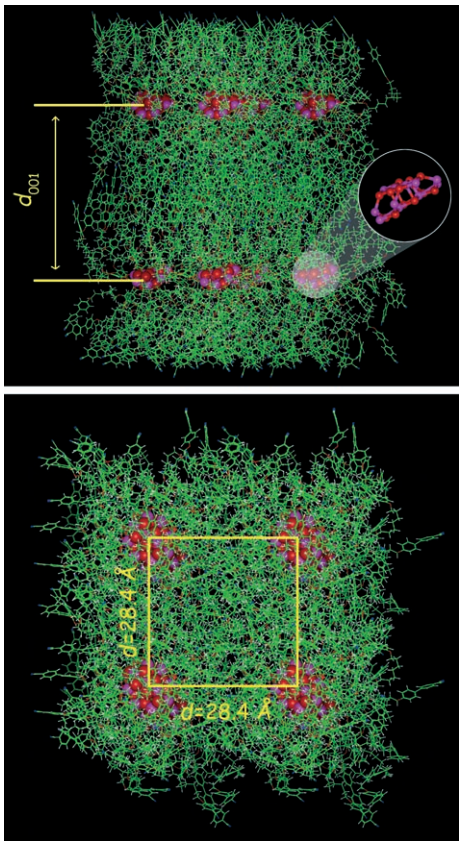

Figure 3. Views of the lamellar packing of the cluster $[Mn_{12}L^3{}_{16}]$. Above: Side view of the lamellar packing of the cyanobiphenyl groups and clusters in the smectic layer. Below: Top view of the in-layer lateral arrangement of the clusters forming a squarelike lattice.

carboxylates) are organized in a hexagonal array within the smectic phase;[26] the carboxylates are organized in the layers of the calamitics with or without correlation between the layers (filled mesh phases with random, 3D rhombohedral and channelled-layer suborganizations). Here, the Mn_{12} clusters are squarely packed in the alkyl sublayers, with no long-range correlation between the layers, and can also accordingly be described as a filled, random mesh smectic phase.

Thus, to summarize, we report for the first time the synthesis and characterization of Mn_{12} clusters forming fluid mesophases with 3D (cubic) or 1D (smectic) positional order. Even though it is short-ranged, the intralayer ordering of the molecular cores in the smectic phase is nevertheless square-like. The magnetic properties are preserved upon functionalization, and the molecules are thermally stable up to 150 °C. Moreover, the main molecular axes of the magnetic cores, which coincide with the magnetic easy axes below T_B (i.e. 2 K), share a common alignment direction in a nematic sense. It seems reasonable to expect that these qualities might facilitate the 2D ordering of these clusters on surfaces, which is the ultimate goal. The self-organization on a surface could possibly be obtained from a solution process or by thermal evaporation. We are currently modifying the ligand structure and the regioselective substitution of two different ligands (at the axial and equatorial positions) to tailor more precisely the mesomorphic behavior of these SMMs.[27]

Received: September 27, 2007
Published online: November 28, 2007

Keywords: cluster compounds · liquid crystals · magnetic properties · metallomesogens · self-assembly

[1] "Single-Molecule Magnets and Related Phenomena": *Struct. Bonding (Berlin)* **2006**, *122* (Ed.: R. Winpenny).
[2] a) R. Sessoli, *Mol. Cryst. Liq. Cryst.* **1995**, *274*, 145–147; b) D. Gatteschi, R. Sessoli, *Angew. Chem.* **2003**, *115*, 278–309; *Angew. Chem. Int. Ed.* **2003**, *42*, 268–297, and references therein; c) A. Caneschi, D. Gatteschi, R. Sessoli, *J. Am. Chem. Soc.* **1991**, *113*, 5873–5874.
[3] a) S. Osa, T. Kido, N. Matsumoto, N. Re, A. Pochaba, J. Mrozinski, *J. Am. Chem. Soc.* **2004**, *126*, 420–421; b) C. M. Zaleski, E. C. Depperman, J. W. Kampf, M. L. Kirk, V. L. Pecoraro, *Angew. Chem.* **2004**, *116*, 4002–4004; *Angew. Chem. Int. Ed.* **2004**, *43*, 3912–3914.
[4] R. E. P. Winpenny, *J. Chem. Soc. Dalton Trans.* **2002**, 1–10.
[5] D. Gatteschi, R. Sessoli, A. Cornia, *Chem. Commun.* **2000**, 725–732.
[6] T. Kato, N. Mizoshita, K. Kishimoto, *Angew. Chem.* **2006**, *118*, 44–74; *Angew. Chem. Int. Ed.* **2006**, *45*, 38–68.
[7] a) N. Tirelli, F. Cardullo, T. Habicher, U. W. Suter, F. Diederich, *J. Chem. Soc. Perkin Trans. 2* **2000**, 193–198; b) R. Deschenaux, B. Donnio, D. Guillon, *New J. Chem.* **2007**, *31*, 1064–1073.
[8] a) E. Terazzi, S. Suarez, S. Torelli, H. Nozary, D. Imbert, O. Mamula, J.-P. Rivera, E. Guillet, J.-M. Bénech, G. Bernardinelli, R. Scopelliti, B. Donnio, D. Guillon, J.-C. G. Bünzli, C. Piguet, *Adv. Funct. Mater.* **2006**, *16*, 157–168; b) T. Cardinaels, K. Driesen, T. N. Parac-Vogt, B. Heinrich, C. Bourgogne, D. Guillon, B. Donnio, K. Binnemans, *Chem. Mater.* **2005**, *17*, 6589–6598.
[9] a) R. W. Date, E. Fernandez Iglesias, K. E. Rowe, J. M. Elliott, D. W. Bruce, *Dalton Trans.* **2003**, 1914–1931; b) F. Camerel, R. Ziessel, B. Donnio, D. Guillon, *New J. Chem.* **2006**, *30*, 135–139.
[10] a) I. Aprahamian, T. Yasuda, T. Ikeda, S. Saha, W. R. Dichtel, K. Isoda, T. Kato, J. F. Stoddart, *Angew. Chem.* **2007**, *119*, 4759–4763; *Angew. Chem. Int. Ed.* **2007**, *46*, 4675–4679; b) E. D. Baranoff, J. Voignier, T. Yasuda, V. Heitz, J.-P. Sauvage, T. Kato, *Angew. Chem.* **2007**, *119*, 4764–4767; *Angew. Chem. Int. Ed.* **2007**, *46*, 4680–4683.
[11] J. Gómez-Segura, J. Veciana, D. Ruiz-Molina, *Chem. Commun.* **2007**, 3699–3707.
[12] Crystal data: $C_{160}H_{176}Mn_{12}O_{96}$, $M_r = 4523.61\ g\,mol^{-1}$, triclinic, space group $P\bar{1}$, $a = 18.539(2)$, $b = 24.383(5)$, $c = 26.353(5)$ Å, $\alpha = 86.707(10)$, $\beta = 85.951(10)$, $\gamma = 71.008(10)°$, $V = 11228(2)$ Å^3, $Z = 2$, $\rho_{calcd} = 1.338\ g\,cm^{-3}$, $\lambda(Mo_{K\alpha}) = 0.71073$ Å, $\mu = 0.714\ mm^{-1}$, $T = 173(2)$ K, $1.39° < \theta < 30.05°$, h,k,l: 0/26, −31/34, −29/26, a total of 52992 reflections collected and 34401 reflections with $I > 2\sigma(I)$, 2565 parameters refined, $R_1 = 0.0611$, $R_2 = 0.1028$, $wR_2 = 0.1696$, GooF = 1.243. CCDC-651104 contains the supplementary crystallographic data for this paper. These data can be obtained free of charge from The Cambridge Crystallographic Data Centre via www.ccdc.cam.ac.uk/data_request/cif.
[13] a) T. Lis, *Acta Crystallogr Sect. B* **1980**, *36*, 2042–2046; b) S. M. J. Aubin, Z. Sun, I. A. Guzei, A. L. Rheingold, G. Christou, D. N. Hendrickson, *Chem. Commun.* **1997**, 2239–2240; c) R. Sessoli, H.-L. Tsai, A. R. Schake, S. Wang, J. B. Vincent, K. Folting, D. Gatteschi, G. Christou, D. N. Hendrickson, *J. Am. Chem. Soc.* **1993**, *115*, 1804–1816; d) S. M. J. Aubin,

Z. Sun, H. J. Eppley, E. M. Rumberger, I. A. Guzei, K. Folting, P. K. Gantzel, A. L. Rheingold, G. Christou, D. N. Hendrickson, *Inorg. Chem.* **2001**, *40*, 2127 – 2146.
[14] a) M. A. Novak, R. Sessoli, A. Caneschi, D. Gatteschi, *J. Magn. Magn. Mater.* **1995**, *146*, 211 – 213; b) R. Sessoli, D. Gatteschi, A. Caneschi, M. A. Novak, *Nature* **1993**, *365*, 141 – 143.
[15] a) K. Takeda, K. Awaga, T. Inabe, *Phys. Rev. B* **1998**, *57*, R11062; b) J. An, Z.-D. Chen, J. Bian, J.-T. Chen, S.-X. Wang, S. Gao, G.-X. Xu, *Inorg. Chim. Acta* **2000**, *299*, 28 – 34.
[16] D. Ruiz-Molina, P. Gerbier, E. Rumberger, D. B. Amabilino, I. A. Guzei, K. Folting, J. C. Huffman, A. Rheingold, G. Christou, J. Veciana, D. N. Hendrickson, *J. Mater. Chem.* **2002**, *12*, 1152 – 1161.
[17] a) K. Takeda, K. Awaga, *Phys. Rev. B* **1997**, *56*, 14560 – 14565; b) K. Awaga, Y. Suzuki, H. Hachisuka, K. Takeda, *J. Mater. Chem.* **2006**, *16*, 2516 – 2521.
[18] C. Hammond in *The Basics of Crystallography and Diffraction*, 2nd ed., IUCr, Oxford Science Publications, Oxford, **2001**.
[19] a) C. Tschierske, *J. Mater. Chem.* **1998**, *8*, 1485 – 1508; b) D. J. P. Yeardley, G. Ungar, V. Percec, M. N. Holerca, G. Johansson, *J. Am. Chem. Soc.* **2000**, *122*, 1684 – 1689; c) H. Duan, S. D. Hudson, G. Ungar, M. N. Holerca, V. Percec, *Chem. Eur. J.* **2001**, *7*, 4134 – 4141; d) I. Bury, B. Heinrich, C. Bourgogne, D. Guillon, B. Donnio, *Chem. Eur. J.* **2006**, *12*, 8396 – 8413.
[20] a) S. Diele, *Curr. Opin. Solid State Mater. Sci.* **2002**, *6*, 333 – 342; b) S. Kutsumizu, *Curr. Opin. Solid State Mater. Sci.* **2002**, *6*, 537 – 543.
[21] a) A. M. Levelut, M. Clerc, *Liq. Cryst.* **1998**, *24*, 105 – 115; b) M. Impéror-Clerc, *Curr. Opin. Colloid Interface Sci.* **2005**, *9*, 370 – 376; c) X. Zeng, G. Ungar, M. Impéror-Clerc, *Nat. Mater.* **2005**, *4*, 562 – 567.
[22] B. Donnio, S. Buathong, I. Bury, D. Guillon, *Chem. Soc. Rev.* **2007**, *36*, 1495 – 1513.
[23] a) D. Guillon, A. Skoulios, *Mol. Cryst. Liq. Cryst.* **1983**, *91*, 341 – 352; b) F. Hardouin, A. M. Levelut, M. F. Achard, G. Sigaud, *J. Chim. Phys.* **1983**, *80*, 53 – 64.
[24] A. De Vries, *J. Chem. Phys.* **1979**, *71*, 25 – 31.
[25] C. Tschierske, *Chem. Soc. Rev.* **2007**, DOI: 10.1039/b615517k.
[26] B. Chen, X. B. Zeng, U. Baumeister, S. Diele, G. Ungar, C. Tschierske, *Angew. Chem.* **2004**, *116*, 4721 – 4725; *Angew. Chem. Int. Ed.* **2004**, *43*, 4621 – 4625.
[27] C. Boskovic, M. Pink, J. C. Huffman, D. N. Hendrikson, G. Christou, *J. Am. Chem. Soc.* **2001**, *123*, 9914 – 9915.

